

# Pyrolysis of Acrylonitrile at Elevated Temperatures. Studies with a Single-Pulse Shock Tube

Assa Lifshitz,\* Menashe Bidani, Aya Suslensky, and Carmen Tamburu

Department of Physical Chemistry, The Hebrew University, Jerusalem 91904, Israel (Received: April 25, 1988; In Final Form: July 18, 1988)

The thermal decomposition of acrylonitrile was studied behind reflected shocks in a single-pulse shock tube over the temperature range 1150–1430 K and overall densities of  $\sim 3 \times 10^{-5}$  mol/cm<sup>3</sup>. Under these conditions the major reaction products are (1) hydrogen cyanide and acetylene and (2) hydrogen and cyanoacetylene:  $\text{CH}_2=\text{CHCN} \rightarrow \text{CH}\equiv\text{CH} + \text{HCN}$  (reaction 1) and  $\text{CH}_2=\text{CHCN} \rightarrow \text{CH}\equiv\text{C}-\text{CN} + \text{H}_2$  (reaction 7). In the presence of toluene, at a ratio of  $[\text{toluene}]_0/[\text{acrylonitrile}]_0 \sim 10/1$ , a twofold decrease in the production rate of these products was observed, indicating a free-radical mechanism in parallel to the four-center eliminations. After the contribution of the free radical chain was subtracted, the following rate constants for the four-center eliminations were obtained:  $k_1 = 10^{12.25} \exp(-68 \times 10^3/RT) \text{ s}^{-1}$ , and  $k_2 = 10^{13.40} \exp(-77 \times 10^3/RT) \text{ s}^{-1}$ , where activation energies are expressed in units cal/mol. Ethylene was found in quantities roughly equal to those of cyanoacetylene.  $\text{C}_2\text{N}_2$ ,  $\text{CH}_3\text{CN}$ ,  $\text{CH}_4$ ,  $\text{C}_4\text{H}_6$ , and  $\text{C}_2\text{H}_6$  were found in the postshock mixtures but at much lower concentrations. Arrhenius parameters for the formation rate of the different reaction products are given and the general pyrolysis mechanism is discussed.

## Introduction

Aliphatic nitriles, in particular acetonitrile and acrylonitrile, are generated when nitrogen-containing heterocyclics and polymers such as polyacrylonitrile and polyurethane are exposed to fire.<sup>1</sup> Upon their formation these nitriles decompose and produce poisonous gases among which hydrogen cyanide is the main product. It is now well established that the inhalation of these gases in fire environments is an important contributor to fire fatalities.<sup>2</sup>

Compared to the large volume of data obtained on hydrocarbon reactions both under pyrolytic and oxidative environments, relatively little effort has been devoted to kinetic studies of the pyrolysis of organic nitriles and of nitrogen-containing molecules in general.

Eliminations of hydrogen cyanide from ethyl, isopropyl, *tert*-butyl and cyclobutyl cyanides have been studied.<sup>3–8</sup> Rate constants for the assumed four-center eliminations were deduced but no information on the distribution of other products in the reaction was reported. The decomposition of acetonitrile was studied in more detail by two groups of investigators<sup>9,10</sup> and recently in this laboratory.<sup>11</sup> The main products of the decomposition were methane and hydrogen cyanide, both formed by a free-radical mechanism. Recently the high-temperature pyrolyses of other two nitrogen-containing molecules, pyrrolidine<sup>12</sup> and pyrrole,<sup>13</sup> were studied. Hydrogen cyanide was the main product but a plethora of other products was also found.

We are not aware of any kinetic study on the high-temperature pyrolysis of acrylonitrile even though polyacrylonitrile is an important polymer. We report in this article a single-pulse shock tube investigation of acrylonitrile pyrolysis. The distribution of reaction products and the Arrhenius parameters for the rate of their production are reported and a discussion of the pyrolysis mechanism is presented.

## Experimental Section

*A. Apparatus.* The thermal decomposition of acrylonitrile was studied behind reflected shocks in a pressurized driver, 52 mm i.d. single-pulse shock tube. The tube and its mode of operation have been described in a recent publication<sup>11</sup> and will be discussed here only very briefly. The driven section was 4 m long and divided in the middle by a 52 mm i.d. ball valve. The driver had a variable length up to a maximum of 2.7 m and could be varied in small steps in order to obtain the most rapid cooling conditions. A 36-L dump tank was connected to the driven section near the diaphragm holder in order to prevent reflection of transmitted shocks and to reduce the final pressure in the tube. The driven section was separated from the driver by Mylar polyester film of various thicknesses depending upon the desired shock strength.

After pumping down the tube to approximately  $10^{-5}$  Torr, the reaction mixture was introduced into the section between the 52 mm i.d. ball valve and the end plate and pure argon into the section between the diaphragm and the valve, including the dump tank. After firing the shock, gas samples were collected from the tube through an outlet in the driven section (near the end plate) in 150-cm<sup>3</sup> glass bulbs and analyzed on a Hewlett-Packard Model 5890A gas chromatograph using flame ionization and NPD detectors.

Reflected shock parameters were calculated from the measured incident shock velocities using the three conservation equations and the ideal gas equation of state. The molar enthalpies of acrylonitrile were taken from Stull et al.<sup>14</sup>

The incident shock velocities were measured with two miniature, high-frequency pressure transducers (Vibrometer Model 6QP500) placed 300 mm apart near the end plate of the driven section. The signals generated by the shock wave passing over the transducers were fed through a home-built piezo amplifier to a Nicolet Model 3091 digital oscilloscope. Time intervals between the two signals shown on the oscilloscope were obtained digitally with an accuracy of  $2 \mu\text{s}$  (out of about 450), corresponding to approximately 15 K. A third transducer (P.C.B. Model 113A26) placed in the center of the end plate, provided measurements of the reaction dwell times (approximately 1.8 ms) with an accuracy of  $\sim 5\%$ . Cooling rates were approximately  $5 \times 10^5$  K/s.

*B. Materials and Analysis.* A reaction mixture containing 1% acrylonitrile in argon was prepared and stored at high pressure in a stainless steel cylinder. Both the cylinder and the line were

(1) Woolley, W. D.; Ames, S. A.; Fardell, P. J. *Fire Mater.* **1979**, *3*, 110.  
(2) Anderson, R. A.; Watson, A. A.; Harland, W. A. *Med. Sci. Law* **1981**, *21*, 288.

(3) King, K. D.; Goddard, R. D. *Int. J. Chem. Kinet.* **1975**, *7*, 109, 837.

(4) King, K. D.; Goddard, R. D. *J. Am. Chem. Soc.* **1975**, *97*, 4504.

(5) King, K. D.; Goddard, R. D. *J. Phys. Chem.* **1976**, *80*, 546.

(6) King, K. D.; Goddard, R. D. *J. Phys. Chem.* **1978**, *82*, 1675.

(7) Dastoor, P. N.; Emovon, E. U. *Can. J. Chem.* **1973**, *51*, 366.

(8) Hunt, M.; Kerr, J. A.; Trotman-Dickenson, A. F. *J. Chem. Soc.* **1965**, 5074.

(9) Asmus, T. W.; Houser, T. J. *J. Phys. Chem.* **1969**, *73*, 2555.

(10) Metcalfe, E.; Booth, D.; McAndrew, H.; Woolley, W. D. *Fire Mater.* **1983**, *7*, 185.

(11) Lifshitz, A.; Moran, A.; Bidani, S. *Int. J. Chem. Kinet.* **1987**, *19*, 61.

(12) Lifshitz, A.; Agranat, A.; Bidani, M.; Suslenski, A. *J. Phys. Chem.* **1987**, *91*, 6043.

(13) Lifshitz, A.; Suslenski, A.; Tamburu, C., unpublished results.

(14) Stull, D. R.; Westrum, Jr., E. F.; Sinke, G. C. *The Chemical Thermodynamics of Organic Compounds*; Wiley: New York, 1969.

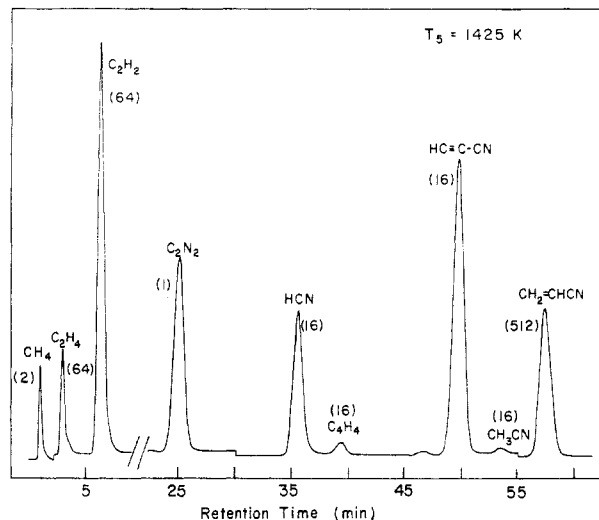


**Figure 1.** A gas chromatogram of a postshock mixture of 1% acrylonitrile in argon at 1425 K. The chromatogram is obtained on a Porapak N column using an FID. The numbers on the peaks indicate attenuation factors.

pumped down to better than  $10^{-5}$  Torr before the preparation of the mixture.

The acrylonitrile was obtained from B.D.H. Chemicals Ltd. and showed only one GC peak. The toluene used was A.R. grade obtained from Frutarum Chemical Co. The argon used was Matheson ultra-high-purity grade, listed as 99.9995%, and the helium was Matheson pure grade listed as 99.999%. All materials were used without further purification.

Gas analyses of the postshock samples were performed on a 2-m Porapak N column. Its initial temperature of 35 °C was gradually elevated to 150 °C in an analysis which lasted about an hour. A typical chromatogram of 1% acrylonitrile in argon shock heated to 1425 K is shown in Figure 1.

We were unable to analyze hydrogen quantitatively in the GC (using a TCD) because of the presence of relatively large quantities of helium trapped in the postshock mixtures. Since hydrogen is eluted immediately after the helium, its peak rides on the helium peak's tail, preventing a quantitative analysis.

The identification of reaction products was based on GC retention times assisted by ZAB-2F GC/MS measurements. The sensitivities of the various products to the GC detectors were determined relative to acrylonitrile from standard mixtures. The areas under the GC peaks were integrated by a Spectra Physics Model SP4200 computing integrator. The information accumulated on the integrator was transferred after each analysis to an Apple IIe in order to remove spurious peaks and noise and then to a CDC CYBER 185/855 computer for data reduction and graphical presentation.

### Data Reduction and Results

**A. Evaluation of Product Concentrations.** Evaluation of the absolute concentrations of the various reaction products from the GC peak areas was done in the following manner:

1. The concentration of acrylonitrile behind the reflected shock prior to decomposition,  $C_5(\text{acrylonitrile})_0$ , is given by

$$C_5(\text{acrylonitrile})_0 = \{p_1 \times \%(\text{acrylonitrile})\rho_5/\rho_1\}/100RT_1 \quad (\text{I})$$

where  $p_1$  is the pressure in the tube prior to shock heating,  $\%(\text{acrylonitrile})$  is the percent of acrylonitrile in the original mixture,  $\rho_5/\rho_1$  is the compression of the sample behind the reflected shock, and  $T_1$  is room temperature.

2. The concentration of acrylonitrile behind the reflected shock prior to decomposition in terms of its peak area,  $A(\text{acrylonitrile})_0$  is given by

$$A(\text{acrylonitrile})_0 = A(\text{acrylonitrile})_i + 0.5\sum\{N(\text{pr}_i)A(\text{pr}_i)_i/S(\text{pr}_i)\} \quad (\text{II})$$

where  $A(\text{acrylonitrile})_i$  is the peak area of acrylonitrile in the

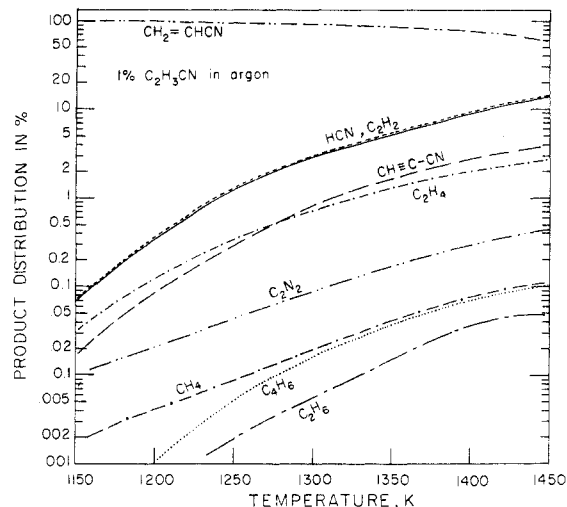


**Figure 2.** Product distribution in postshock mixtures of 1% acrylonitrile in argon shown over the temperature range covered in this investigation. The major products are (1) acetylene and hydrogen cyanide and (2) cyanoacetylene (and hydrogen).

shocked sample,  $A(\text{pr}_i)$ , is the peak area of a product  $i$  in the shocked sample,  $S(\text{pr}_i)$  is its sensitivity relative to acrylonitrile, and  $N(\text{pr}_i)$  is the number of its carbon atoms not including the CN group. The latter does not decompose in the temperature range of this study and can therefore be excluded from the carbon mass balance.

3. The concentration of a product  $i$  in the shocked sample is then given by

$$C_5(\text{pr}_i) = A(\text{pr}_i)_i/S(\text{pr}_i)\{C_5(\text{acrylonitrile})_0/A(\text{acrylonitrile})_0\} \quad (\text{III})$$

Since  $A(\text{acrylonitrile})_0$  is not available in the postshock analysis (only  $A(\text{acrylonitrile})_i$  is), its value must be calculated using eq II.

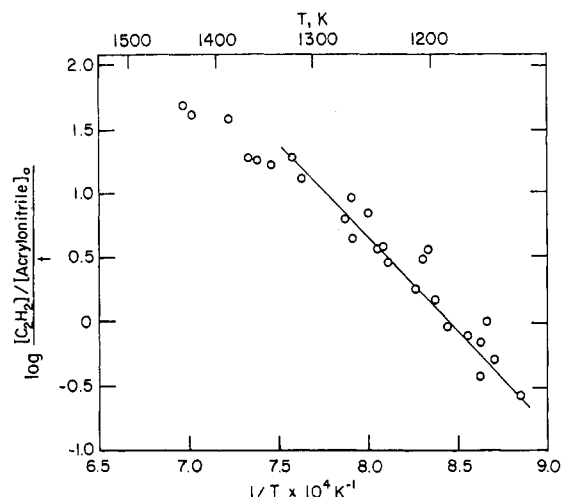
**B. The Distribution of Reaction Products.** In order to determine the production rates of the various products and their dependence on the temperature, some 30 tests with 1% acrylonitrile in argon were run, covering the temperature range 1150–1430 K.

Figure 2 shows the product distribution obtained in the shocked samples over this temperature range. The percent of a given product out of the total shown in the figure corresponds to its mole fraction,  $100C_i/\sum C_i$ , irrespective of the number of its carbon atoms. (Molecular hydrogen is not included.) The major reaction products are hydrogen cyanide and acetylene, which have practically the same concentration over the entire temperature range. Cyanoacetylene is the third major product. Its concentration (somewhat higher than that of ethylene) is by a factor of about 4–5 lower than that of acetylene. Several other reaction products appear in the postshock mixtures but at much lower concentration. The mechanism of their production will be later discussed.

**C. Arrhenius Rate Parameters.** In Figures 3–6, the production rates of  $\text{CH}\equiv\text{CH}$ ,  $\text{HCN}$ ,  $\text{CH}\equiv\text{C}-\text{CN}$ , and  $\text{CH}_2=\text{CH}_2$  defined as

$$\text{rate}(\text{pr}_i) = C_5(\text{pr}_i)_i/t \quad (\text{IV})$$

and divided by the initial acrylonitrile concentration are plotted against reciprocal temperature. They are expressed in units of  $\text{s}^{-1}$  and at low extents of reaction can be considered as first-order rate constants. Toward the end of the high-temperature range a slight bend in the lines shows up owing to the depletion of the reactant and due to subsequent reactions of the products. Values of  $E$  in units of kcalories per mole obtained from the slopes of the lines and their corresponding preexponential factors are summarized in Table I. Although the points on the figures are calculated as first-order rate constants they do not necessarily represent elementary unimolecular reactions. The Arrhenius temperature dependences and preexponential factors that are



**Figure 3.** A plot of  $\log \{[C_2H_2]_t/[acrylonitrile]_0\}/t$  against the reciprocal temperature. The slope of the line gives the Arrhenius activation energy for the major reaction:  $CH_2=CHCN \rightarrow CH\equiv CH + HCN$ .  $E = 68$  kcal/mol.

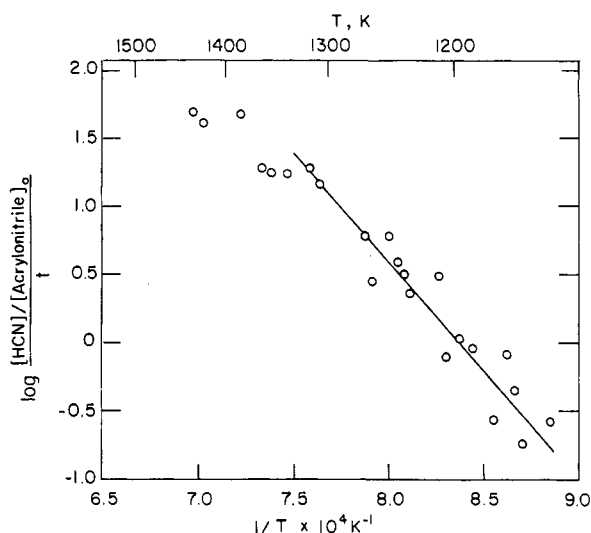


**Figure 4.** A plot of  $\log \{[HCN]_t/[acrylonitrile]_0\}/t$  against the reciprocal temperature. The line corresponds to the first-order rate constant of the major reaction:  $CH_2=CHCN \rightarrow CH\equiv CH + HCN$  with practically the same Arrhenius parameters obtained in Figure 3.

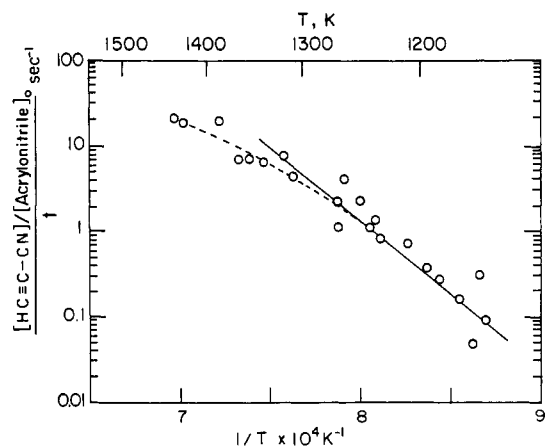


**Figure 5.** A plot of  $\log \{[CH\equiv C-CN]_t/[acrylonitrile]_0\}/t$  against the reciprocal temperature. The slope of the line on the figure corresponds to an activation energy of 77 kcal/mol for the reaction  $CH_2=CHCN \rightarrow CH\equiv C-CN + H_2$ .

obtained from these figures can serve as a basis for computer modeling of the decomposition scheme, when the rate parameters of the elementary reactions that participate in the decomposition become available.

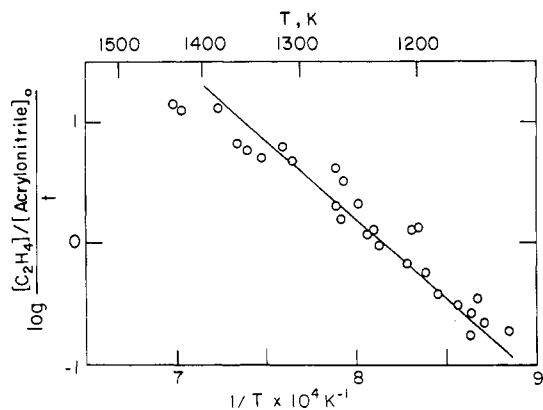


**Figure 6.** A plot of  $\log \{[C_2H_4]_t/[acrylonitrile]_0\}/t$  vs  $1/T$ . Ethylene is obtained by an abstraction reaction between the  $CH_2=CH$  radical and acrylonitrile.

**TABLE I: Preexponential Factors ( $A$ ) and Arrhenius Temperature Dependences ( $E$ ) for the First-Order Rate Constants of Formation of the Various Products**

compound	$\log A, s^{-1}$	$E, kcal/mol$	$T, K$
$C_2H_2, HCN$	12.25	68	1140-1340
$CH\equiv C-CN$	13.40	77	1140-1340
$C_2H_4$	10.61	60	1140-1340
$C_2N_2$	9.13	56	1160-1380
$C_4H_6$	12.44	81	1200-1400
$CH_2=CHCN^a$	12.28	67	1140-1340

<sup>a</sup> First-order rate constant for the overall decomposition of acrylonitrile.

### Pyrolysis Mechanism and Reaction Scheme

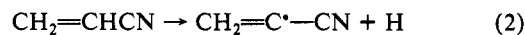
**A. Major Reaction Products.** As can be seen in Figure 2, acetylene and hydrogen cyanide are the major products in the pyrolysis and appear in almost equal concentrations over the entire temperature range of this investigation. Having the same concentration, their production can be attributed to the stoichiometric reaction



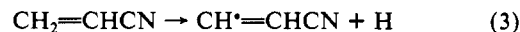
The question whether this reaction is an elementary unimolecular step or alternatively takes place via a free-radical chain reaction must still be clarified since the production of these two species can be described also by the chain



where H atoms come from the self-dissociation of acrylonitrile:

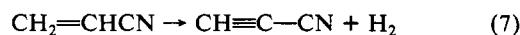


or

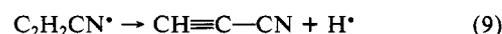


no matter how slow these reactions might be.

A similar argument holds also for the production mechanism of cyanoacetylene and hydrogen. Their production is attributed to the stoichiometric reaction



which can be an elementary unimolecular reaction but may as well take place via



The possibility that both reaction channels, the unimolecular and the free radical, operate simultaneously does also exist.

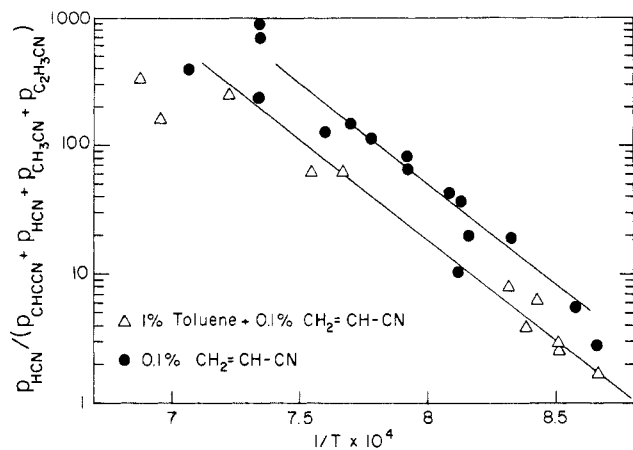


**Figure 7.** The logarithm of the GC peak height of HCN ( $P_{\text{HCN}}$ ) divided by the peak heights of acrylonitrile and all the CN containing products is plotted vs  $1/T$  for experiments with and without toluene. The factor of  $\sim 2$  difference between the two series of experiments suggests a contribution of a free-radical mechanism in the reaction:  $\text{CH}_2=\text{CHCN} \rightarrow \text{CH}\equiv\text{CH} + \text{HCN}$ .

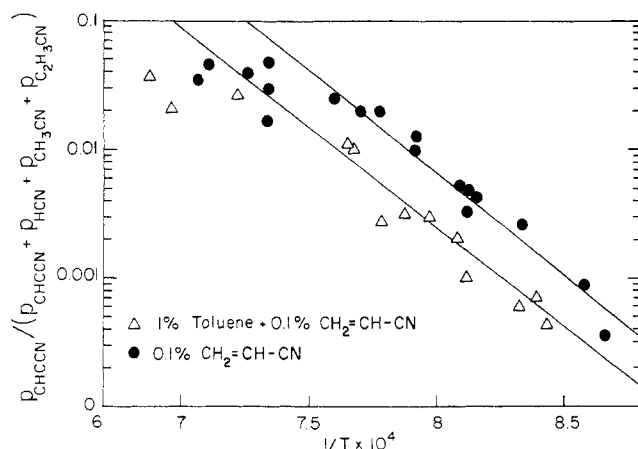


**Figure 8.** The logarithm of the GC peak height of  $\text{CH}=\text{CCN}$  ( $P_{\text{CH}=\text{CCN}}$ ) divided by the peak heights of acrylonitrile and all the CN containing products is plotted vs  $1/T$  for experiments with and without toluene. The factor of  $\sim 2$  difference between the two series of experiments suggests a contribution of a free-radical mechanism in the reaction  $\text{CH}_2=\text{CHCN} \rightarrow \text{CH}=\text{C}-\text{CN} + \text{H}_2$ .

In order to clarify this question a series of experiments were run in which 1% toluene was added to the reaction mixture at a ratio of  $[\text{toluene}]_0/[\text{acrylonitrile}]_0 \approx 10/1$  in order to suppress the free-radical reactions (if they exist). A series of experiments with 0.1% acrylonitrile in argon without toluene was also run for comparison. In these two series of experiments we analyzed only for the nitrogen-containing species using NPD. (Since some acetylene is produced by the pyrolysis of the toluene itself, the comparison of the acetylene concentration with and without toluene is questionable.) The results of these studies are shown in Figures 7 and 8. As can be seen the concentrations of both hydrogen cyanide and cyanoacetylene are suppressed by a factor of approximately 2 in the presence of this large quantity of toluene, suggesting that a contribution of a free-radical mechanism does exist. There is no indication, however, that this contribution is temperature dependent, which means that the observed activation energies of reactions 1 and 2 are close to those of the unimolecular four-center eliminations.

The first-order rate constants deduced for the unimolecular eliminations in reactions 1 and 2 are obtained by dividing their overall rates (Figures 3, 4, and 5) by a factor of 2:

$$k_1 = 10^{12.25 \pm 0.4} \exp[-(68 \pm 2) \times 10^3/RT] \text{ s}^{-1}$$

$$k_2 = 10^{13.40} \exp[-77 \times 10^3/RT] \text{ s}^{-1}$$

Since the slopes of the lines which correspond to the production

rates of  $\text{C}_2\text{H}_2$  (Figure 3) and HCN (Figure 4) are different by 4 kcal/mol, the rate parameters for reaction 1 are given with their uncertainties. The values obtained for the preexponential factors clearly suggest rigid transition states, which are compatible with those of numerous unimolecular reactions of the same nature.<sup>7,15</sup>

As has been mentioned before, the only source of free radicals in the system is the self-dissociation of acrylonitrile. One must therefore estimate some average H atom concentration ( $[\text{H}]_{\text{av}}$ ) based on this source (under the conditions of the present experiment) in order to check whether it can support the free-radical path in reaction 1.

As far as we are aware the dissociation rate of acrylonitrile has not been measured in the past. A good estimate would be the dissociation rate of acetonitrile under the same experimental conditions.<sup>11</sup>  $\text{CH}_3\text{CN} \rightarrow \text{CH}_2\text{CN} + \text{H}$ ,  $\{k_{\text{diss}} = 10^{15.79} \exp(-96.6 \times 10^3/RT) \text{ s}^{-1}\}$ .

The average concentration of H atoms can be calculated from the relation  $[\text{H}]_{\text{av}} = k_{\text{diss}}[\text{CH}_2=\text{CHCN}]_0 t^{1/2}$ , where  $k_{\text{diss}}$  is the estimated dissociation rate constant of acrylonitrile,  $[\text{CH}_2=\text{CHCN}]_0$  is its initial concentration, and  $t^{1/2}$  is half of the reaction dwell time. At 1240 K, in the middle of the temperature range of these experiments, one obtains for the concentration of H atoms  $[\text{H}]_{\text{av}} = 1.75 \times 10^{-11} \text{ mol/cm}^3$ .

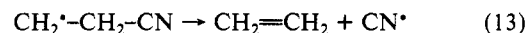
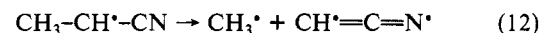
Since the contribution of the free-radical path to reaction 1 is roughly equal to that of the unimolecular elimination, then  $k_{\text{rad}}[\text{H}]_{\text{av}} \approx 10^{12.25} \exp(-68 \times 10^3/RT) \text{ s}^{-1}$ . At 1240 K this yields for  $k_{\text{rad}}$  a value of  $1.0 \times 10^{11} \text{ cm}^3/(\text{mol s})$  which is a very reasonable value for a radical-molecule reaction of this type.

**B. Minor Reaction Products.** Formation of minor products can be accounted for by various free-radical reactions accompanied by decomposition of unstable intermediates.

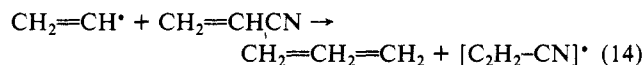
The attachment of a hydrogen atom to acrylonitrile can lead to the production of three different  $\text{C}_2\text{H}_2\text{CN}$  isomers:



which upon their decomposition will produce vinyl, methyl, and CN radicals, respectively.



**a. Vinyl Radicals.** Once vinyl radicals are formed they will react in three different channels to produce acetylene by their unimolecular decomposition (reaction 6), ethylene by an abstraction (reaction 14), and butadiene by recombination (reaction 15):

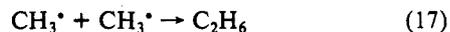
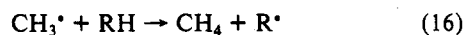


In view of the low concentration of the  $\text{CH}_2=\text{CH}^\bullet$  radical, its recombination is slow compared to its abstraction reactions. This is deduced from the very low concentration of butadiene and the higher concentration of ethylene (Figure 2). The presence of ethylene and butadiene in the postshock mixtures confirms the existence of the  $\text{CH}_2=\text{CH}^\bullet$  radical and supports the interpretation of the results obtained in the presence of toluene.

**b. Methyl Radicals.** The production of methane, acetonitrile, and ethane involves reactions of methyl radicals. The latter can be produced by the decomposition of one of the isomers which is obtained by attachment of hydrogen atom to acrylonitrile

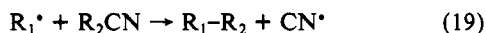
(15) Robinson, P. J.; Holbrook, K. A. *Unimolecular Reactions*; Wiley-Interscience: New York, 1972.

(reaction 12). The reactions that these radicals undergo are



Since all of these compounds are present at very small concentration, the concentration of methyl radicals in the pyrolysis must be small.

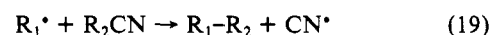
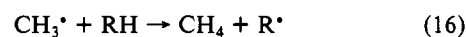
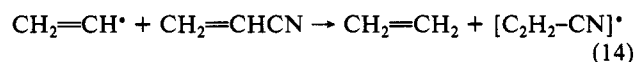
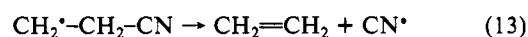
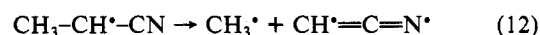
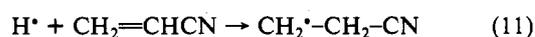
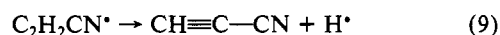
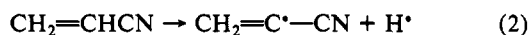
*c. CN Radicals.* Since cyanogen ( $\text{C}_2\text{N}_2$ ) is also found in the postshock mixtures (Figure 1), CN radicals must be present. Their generation in the process of the pyrolysis can take place by reactions of the type



or by reaction 13. Reaction 19 and reaction 13 (which is preceded by reaction 11) are endothermic and can take place only at high temperatures and at a very low rate.

Once a CN radical is formed, an abstraction of an additional CN from either R-CN or HCN to form  $\text{C}_2\text{N}_2$  is exothermic. The presence of cyanogen in the postshock mixture suggests that the endothermicity of reactions 11-13 and 19 does not prevent it from taking place under our experimental conditions. It should be mentioned that cyanogen was also found in small quantities in the pyrolysis of acetonitrile where a similar mechanism for its formation was suggested.<sup>11</sup>

*C. Pyrolysis Scheme.* Based on the discussion just presented, the overall pyrolysis of acrylonitrile can be summarized in the following reaction scheme.



*Acknowledgment.* This research was supported by a grant from Stiftung Volkswagenwerk. We thank Prof. Thomas Just and Dr. Wing Tsang for very valuable discussions.

*Registry No.*  $\text{CH}_2=\text{CHCN}$ , 107-13-1.

## Excited-State Proton-Transfer Processes of *cis*-Dicyanobis(2,2'-bipyridine)ruthenium(II) in Acetonitrile/Water Solvent Systems

Jorge Davila, Carlo Alberto Bigozzi, and Franco Scandola\*

Dipartimento di Chimica dell'Università and Centro di Fotochimica CNR, 44100 Ferrara, Italy  
(Received: May 3, 1988; In Final Form: August 9, 1988)

The excited-state acid-base behavior of *cis*-dicyanobis(2,2'-bipyridine)ruthenium(II),  $\text{Ru}(\text{bpy})_2(\text{CN})_2$ , has been studied in acetonitrile and acetonitrile/water solvent mixtures, with  $\text{HClO}_4$  as the proton source. With respect to water, the use of these solvent systems has several practical advantages (smaller acid concentrations required, better separation and experimental accessibility of successive steps, observation in fluid solution of emission from the monoprotonated form). The ground-state equilibria shift toward lower p*K* values as the water content of the mixed solvent is increased. Depending on the concentration of water, three distinct kinetic regimes for the excited-state proton transfer have been observed. In neat acetonitrile, excited-state deprotonation does not compete with excited-state deactivation, so that emission follows the distribution of variously protonated species present in the ground state. At large (>0.1 M) water concentrations, the proton-transfer steps are fast, and excited-state equilibration is established prior to deactivation, allowing the determination of excited-state p*K* values from emission titration. At low water concentrations (0.01-0.04 M), a hybrid regime is obtained, in which no equilibrium is established in spite of the efficient deprotonation observed. In the excited-state equilibrium regime, the p*K* values depend linearly on the third power of the water concentration, a figure that may be related to the average size of the water clusters solvating the proton.

### Introduction

Proton transfer in electronically excited states (Scheme I) has been actively investigated<sup>1,2</sup> since the original work of Forster<sup>3</sup> and Weller<sup>4</sup> showing that the acidity constant in the excited state,

$*K = *k/k_*$ , can be significantly different from that in the ground state,  $K = k/k_*$ . Most of the work has dealt with singlet and triplet excited states of aromatic molecules in aqueous solution, for which extensive p*K* data have been obtained by using the spectroscopic Forster cycle,<sup>3-6</sup> fluorescence titration,<sup>4,5</sup> or titration of excited-state

(1) Vander Donckt, E. *Prog. React. Kinet.* 1970, 5, 273.

(2) Ireland, J. F.; Wyatt, P. A. H. *Adv. Phys. Org. Chem.* 1976, 12, 131, and references therein.

(3) Forster, Th. *Z. Elektrochem. Angew. Phys. Chem.* 1950, 54, 42, 531.

(4) Weller, A. *Ber. Bunsen-Ges. Phys. Chem.* 1952, 56, 662; 1956, 66, 1144.

(5) Weller, A. *Prog. React. Kinet.* 1961, 1, 189.